Expanding the Constellation-X field of view with Position-Sensitive X-ray Microcalorimeters

E. Figueroa-Feliciano,[a] S. R. Bandler,[b,c] K. Boyce,[b] R. P. Brekosky,[b,d] J. A. Chervenak,[b] F. M. Finkbeiner,[b,e] N. Iyomoto,[b] R. L. Kelley,[b] C. A. Kilbourne,[b] F. S. Porter,[b] T. Saab,[f] and J. E. Sadleir[b,g]

[a]Kavli Institute for Astrophysics and Space Research and the Department of Physics, Massachusetts Institute of Technology, Cambridge, MA 02139, USA;
[b]NASA Goddard Space Flight Center, Greenbelt, MD 20770, USA;
[c]University of Maryland, Department of Astronomy, College Park, MD 20742, USA;
[d]Swales Aerospace, Beltsville, MA 20705, USA;
[e]SSAI, Lanham, MD 20706, USA;
[f]Deptartment of Physics, University of Florida, Gainesville, FL 32611, USA;
[g]Department of Physics, University of Illinois, Urbana, IL 61801, USA

ABSTRACT

We report on our studies of possible configurations for the focal plane of the Constellation-X mission. Taking advantage of new developments in both SQUID multiplexing technology and position-sensitive detectors, we present a viable focal plane intrument design that would greatly enhance the reference Constellation-X configuration of a 32×32 array. An order of magnitude increase in the number of pixels of the focal plane array from the current 1024-pixel reference design is achievable.

Keywords: Constellation-X, X-rays, Microcalorimeters, Position-Sensitive, Transition-Edge Sensor

1. INTRODUCTION

The Constellation-X Mission[1] will be a powerful and revolutionary X-ray observatory. The science case for this mission is well established,[2] and includes the study of the formation and evolution of black holes, cosmology with clusters of galaxies, the growth of structure in the universe, and the life cycles of matter. On most of these observations, the science output of the mission will be significantly enhanced by a larger field of view (FOV) instrument. For cosmology, imaging as much of the cluster as possible with each observation will greatly enhance the capability of the mission, since the limits on cosmology depend on observing many clusters and obtaining their gas density and temperature profiles out to as large a radius as possible. Imaging the first supermassive black holes (active galactic nuclei, or AGN) will require long exposures and obtaining as large a sample as possible will allow statistical studies of the properties of these important objects. For a finite lifetime/observation time, the number of faint AGN detected by Constellation-X will scale as the square of the FOV of the instrument. Studies of the inter-galactic and inter-stellar media will also benefit from larger FOV, as will the number of serendipitous sources discovered throughout the lifetime of the mission. Figure 1 shows the Chandra Deep Field South[3] 1 Ms observation. This heroic Chandra observation is the equivalent of a 40 ks observation with Constellation-X. However, the advantage of this great increase in collecting area is diluted by the small Con-X FOV. The box in the center marks the 2.6' reference design FOV for Con-X. To map out the Chandra field would require 25 Con-X fields, with a total integration time of 1 Ms. The 10' focal plane instrument proposed in this paper would have 20 times more area than the reference design, increasing by more than an order of magnitude the available depth/FOV phase space of the mission.

High Energy, Optical, and Infrared Detectors for Astronomy II
edited by David A. Dorn, Andrew D. Holland Proc. of SPIE Vol. 6276
627615, (2006) · 0277-786X/06/$15 · doi: 10.1117/12.672257

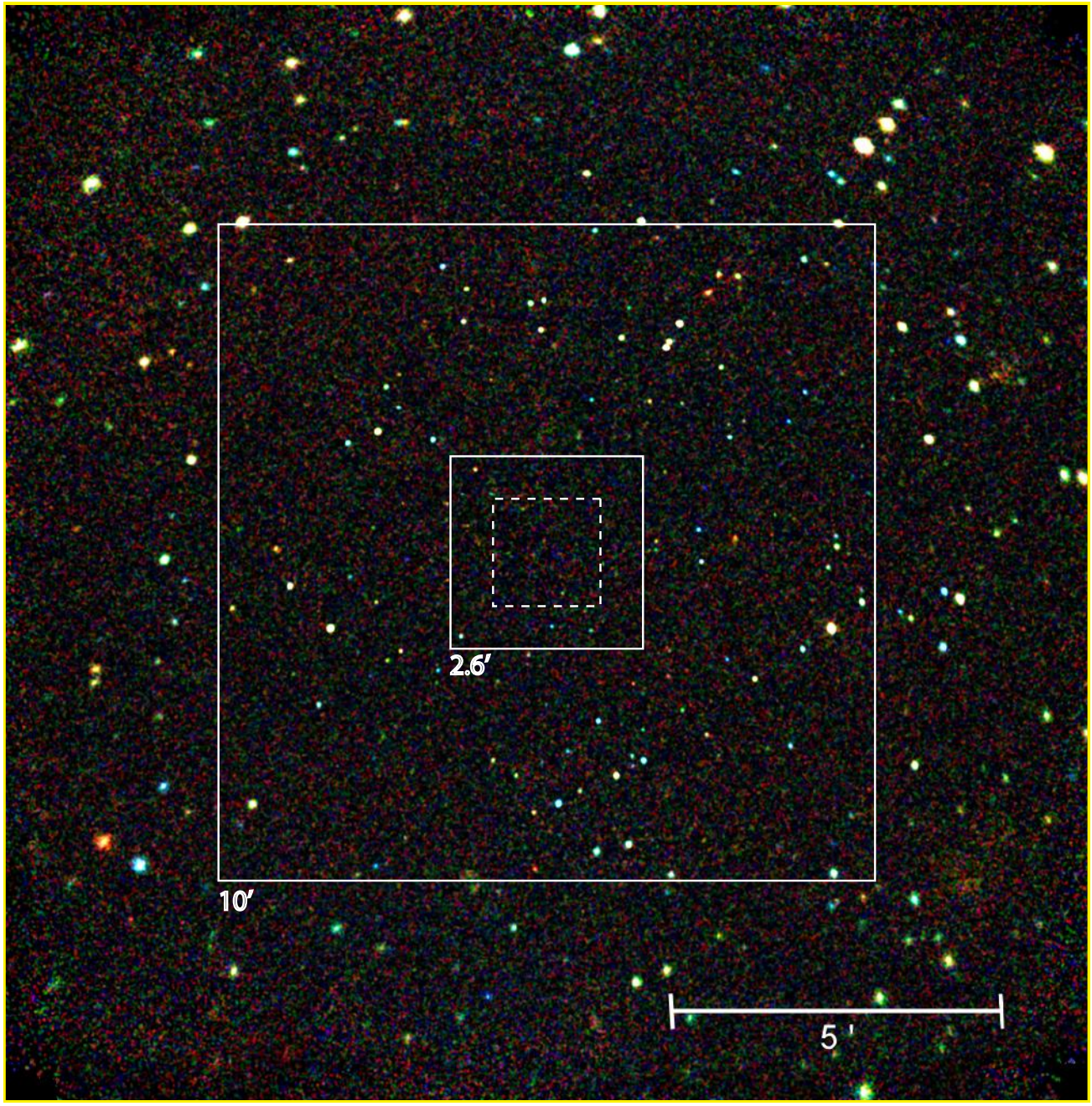

Figure 1. Chandra Deep Field South.[3] The labeled 2.6' box represents the current reference design Constellation-X FOV. The outer 10' box represents the proposed hybrid array's FOV. The dashed line box in the center of the figure represents the inner 20×20 high energy resolution, high throughput, single pixel array. The area outside this box would be populated by an array of Position-Sensitive TESs. The Chandra ACIS-I FOV would require 25 tiled Con-X observations with the reference design's 2.6' Con-X FOV.

Table 1. Contellation-X Baseline Mission Microcalorimeter Characteristics.

Spectral resolving power	$(E/\Delta E) >\sim 300$ from 0.25 keV to 6.0 keV
	1,500 from 6.0 keV to 10 keV
Diameter Field of View	> 2.5 arc min
	$> 30 \times 30$ array (5" pixels)

Table 2. Projected NIST multiplexer capabilities, allowing 10% degradation in energy resolution due to aliased amplifier noise. Taken from Doriese et al.[5]

$\tau_{\pm}$	Max N_{MUX}
1000	196
300	95
50	32

2. THE REFERENCE DESIGN

The current proposed reference design imaging spectrometer for Constellation-X is a 32×32 microcalorimeter array. We are currently developing a transition-edge sensor array with the correct size and quantum efficiency for Constellation-X.[4] We refer the reader to that paper and references therein for a full description of our single-pixel efforts. This array consists of high energy resolution, high-throughput single pixel transition-edge sensors (TESs). A TES is a superconducting thermistor biased in its transition. Small temperature excursions from the quiescent bias point caused by the thermalization of absorbed photons create a large change in resistance which is read out by a SQUID. The array is fabricated lithographically. Each pixel is suspended in individual silicon-nitride membranes to provide the desired thermal decoupling from the silicon substrate, which is thermally anchored to a 50 mK adiabatic demagnetization refrigerator. Micromachined "mushroom" absorbers deposited on the TES allow close packing arrays to be built. These absorbers have overhangs which hide the wiring and membrane structures to form the close-packed focal plane. The time constant of these devices is between 100–300 μs.

Each of these pixels is read out by a SQUID amplifier. These superconducting electonic amplifiers are multiplexed to enable the readout of the full 32×32 array. Our collaborators at the National Institute of Standards and Technology (NIST) recently demonstrated an 8-pixel time-division multiplexer with 3.2 eV FWHM resolution.[5]

3. OPTIMIZING FOR LARGER FOV

The current reference design for the SQUID multiplexer is to have 32 columns of second-stage SQUID amplifiers, each reading out 32 first-stage SQUIDs, one of which is required for each TES in the array. To increase the number of channels from this reference design, it is much less taxing on the overall system complexity and thermal design to increase the number of first-stage SQUIDs per column than to increase the number of columns. The maximum number of SQUIDs per multiplexer column N_{MUX} is a function of the time constant of the microcalorimeter pixels. This is due to the finite bandwidth of the multiplexer, which has to sequentially sample all SQUIDs in a single column ~ 5 faster than the detector time constant. Table 2 shows N_{MUX} for several detector time constants ($\tau_{\pm}$). Slower detector time constants allow more pixels to be read out per SQUID column, increasing the total array FOV.

The time constant of the microcalorimeter directly limits the maximum throughput of the mission. This is due to the fact that a microcalorimeter is a single photon counting device, and for high-resolution energy estimates a minimum time window is needed before another photon can hit the device to allow it to cool back to its quiescent state. We define this time window as $t = f_{hr}\tau$, were τ is the decay time of the device and f_{hr} is a factor that determines the size of the window. This factor is usually somewhere between 10 and 20. Pileup is defined as the condition where two photons hit the detector less than $f_{hr}\tau_{\pm}$ apart from each other. The ability to obtain a high resolution measurement of piled up events is degraded. The amount of degradation depends on

E. Figueroa-Feliciano's e-mail: enectali@mit.edu

Table 3. Mirror and pixel assumptions for this paper.

Mirror point-spread function	Gaussian
Half Power Diameter	10 arcsec
Pixel size	5 arcsec

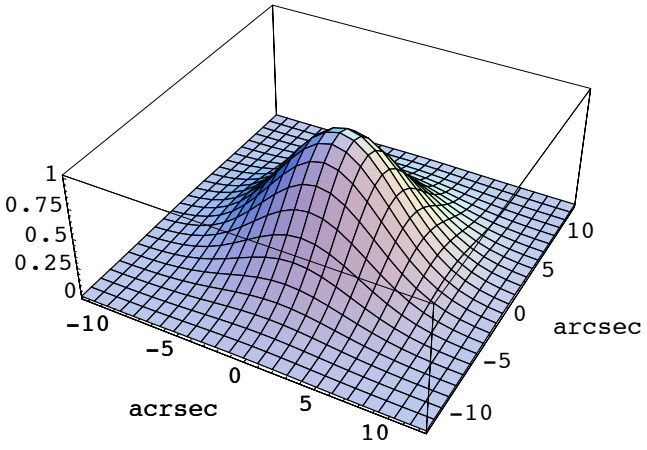

Figure 2. Gaussian PSF with 10 arcsec half-power diameter used for this paper.

how soon after the first photon the second photon is absorbed and the algorithm used to estimate the energy of the photon.

Since photon emission is a stochastic process, at any photon incidence rate there will some fraction of the events which are piled up. The average number of high-resolution events R_{hr} for a given pixel photon rate R_p is

$$R_{hr} = R_p \exp\left(-f_{hr}\tau R_p\right). \tag{1}$$

The telescope optics have a point-spread function (PSF) that distributes the light from a point source into several pixels. Table 3 shows the parameters used for this paper, which are a gaussian PSF with a 10" half-power diameter and 5" pixels. The PSF is shown in Figure 2. Although real PSF distributions are usually more pointed than a gaussian, this distribution is a good enough approximation for the purposes of this paper.

3.1. The need for high-throughput pixels

In this section we calculate the high-resolution fraction for fast single-pixel microcalorimeter arrays under high count rates. Figure 3 shows a 5×5 array of pixels centered on the PSF of our reference design mirror's response to a point source. The middle pixel receives 20% of the photons. The light gray pixels each receive about 8% of the photons, for a total of 64% of the photons in the light gray pixels. The dark gray pixels each receive about 0.9% of the photons, or 16% for all the dark grey pixels. The total number of photons for each area is shown in Table 4.

We have done a simulation of a single-pixel TESs with 100 μs decay times. Figure 4 shows the high resolution fraction of the total number of photons per unit time incident on the array (R_{hr}/R_p) as a function of the count rate R_p. The dashed lines represent the high-res fraction in each of the areas depicted in Figure 3. The high-res fraction goes to 50% of the incident photons at about 5000 counts per second. For Constellation-X, a 1 Crab point source (equal to 2.8×10^{-8} ergs/cm^2/sec in the 2–12 keV band) will have a total count rate of 80,000 counts/sec distributed among the four satellites. That means each microcalorimeter array will receive 20,000 counts per second for a 1 Crab source. So a 100 μs TES array has a 50% high-res fraction for 250 mCrab point

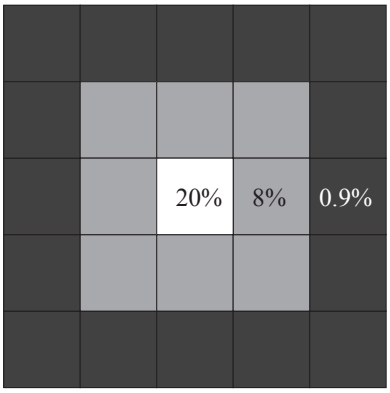

Figure 3. Diagram of inner 5×5 core of single-pixel TES detectors centered on the PSF of a point source. The numbers show how many of the total number of photons hit each pixel. We divide this portion of the array in "rings" around the center pixel. The central pixel (in white) receives 20% of the total photons. The inner light gray ring receives 64% of the photons, and the outer dark gray ring receives 16% of the photons.

Table 4. Distribution of photons from Figure 2 in the 5×5 array shown in Figure 3.

Area	**Photons per pixel**	**Photons per area**
White	20%	20%
Light gray	8%	64%
Dark gray	0.9%	16%

sources. This simulation demonstrates the need for fast time constant microcalorimeter arrays for bright point sources in Constellation-X. As can be seen in Figure 3, very few photons land on pixels outside of a 5×5 grid centered on the source. The nominal Constellation-X array is a 32×32 array. In the X-ray sky, very bright point sources are rare, and thus there will be at most 1 bright point source in a given Con-X field. Although this simulation clearly shows we want the fastest time constants we can obtain for point sources, it also shows we don't need that hight count rate across the whole array. Taking into account dithering or drift of the telescope a 10×10 "hot core" of fast TES would be sufficient. The smaller the hot core, the more channels are available for the slower outer pixels, and the bigger the total FOV of the instrument. To be conservative, in this paper we assume we use a 20×20 high-throughput core of fast single-pixel TESs.

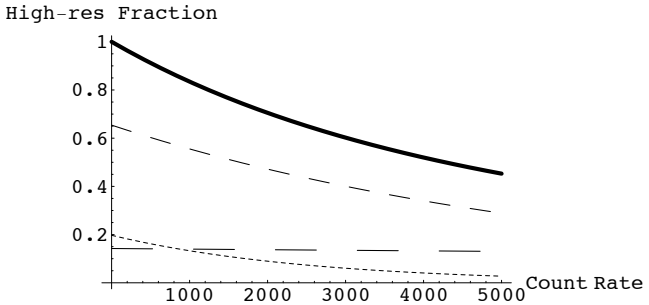

Figure 4. High resolution fraction as a function of count rate. The solid black line is the total high-res fraction for the array. The short-dashed line is the high-res fraction for the central pixel. The medium dashed line is the high-res fraction for the light gray area in Figure 3, and the long-dashed line is the high-res fraction for the dark gray area.

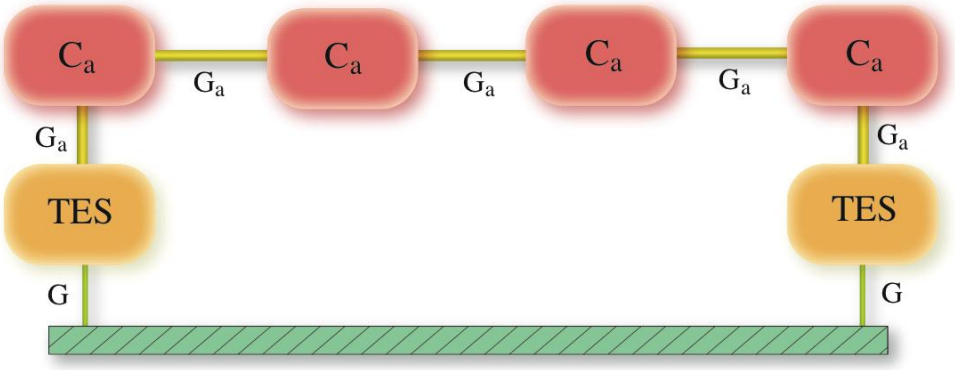

Figure 5. Schematic of a Position-sensitive Transition-edge Sensor (PoST). Several absorber pixels are thermally connected together. A TES at each end of the absorber chain reads out the temperature and is connected to the bath, so any heat deposited in the absorbers has to go through the TESs.

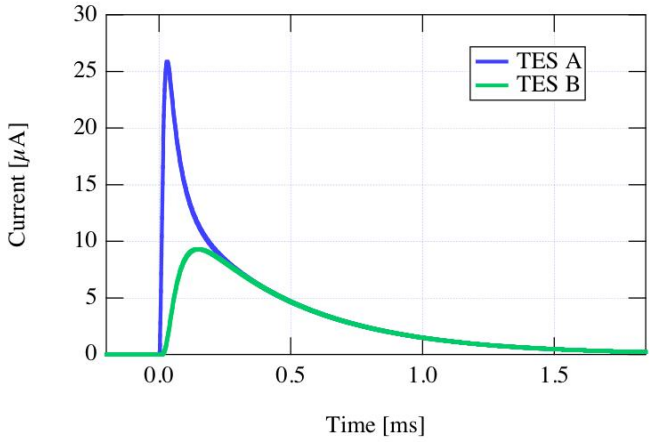

Figure 6. Response of a PoST to a photon absorption. In this model the photon hits an absorber that is closer to one of the TESs. That TES sees a larger initial signal than the farther TES, until the whole PoST comes into equilibrium at about 250 μs and continues to cool. The position of the photon can be determined from this difference, and the energy can be estimated from the sum of the two signals.

3.2. Position-sensitive devices

Apart from bright point sources, the X-ray sky is fairly dim. Extended sources have very low surface brightness, so the number of X-rays on each pixel will be very low. For example, the Perseus Cluster, one of the brightest surface brightness cluster in the sky, has a maximum surface brightness of 2×10^{-14} erg/cm^2/sec/arcsec^2. We estimate that Perseus will have a Constellation-X count rate of 0.014 counts/sec/arcsec^2 at its brightest point (calculated by scaling the relative fluxes of the Crab and Perseus with the Con-X count rate of the Crab). Thus we can design much slower devices for the outer parts of the array that will allow a much large FOV microcalorimeter instrument. We propose to use Position-sensitive Transition-edge Sensors (PoSTs) for this purpose. A schematic of a PoST is shown in Figure 5. A PoST has a series of thermally connected absorbers, with a TES on either end. When a photon is absorbed, the resulting signal in two TESs varies depending on the location of the photon absorption. As seen in Figure 6, the position of the event can be determined by the difference in the two signals, and the sum of the two pulses provides the energy of the X-ray.[6]

To understand what the pileup limitations are of these devices, we simulated an array of PoSTs as shown in Figure 7. Here the PoSTs are aligned vertically, and a point source is centered in the center of the array. Although the PoSTs are assumed to have 10 pixels each, we only show the central 5 in each PoST. The central PoST receives 44% of the photons (assuming the PSF of Figure 2), while the light gray PoSTs each receive 24%

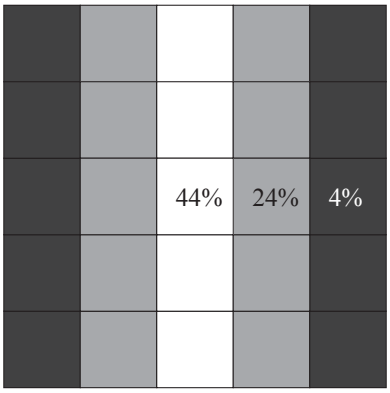

Figure 7. Array of PoSTs with a point source centered on middle PoST. The PoSTs are arranged vertically, so each column of absorbers is an individual PoST. Although the PoSTs we are simulating have 10 absorbers each, we only show the middle 5. The calculated percentage of photons that hit each PoST is shown.

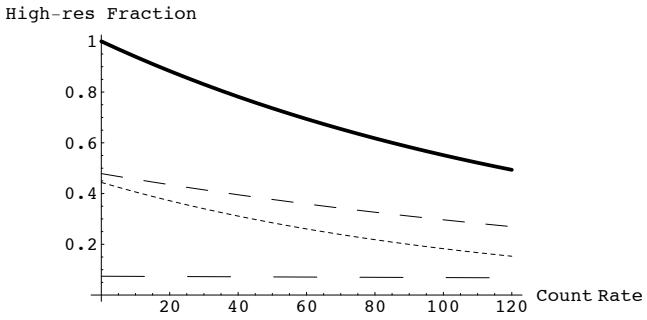

Figure 8. High resolution fraction as a function of count rate for the PoST array shown in Figure 7. The solid black line is the total high-res fraction for the array. The short-dashed line is the high-res fraction for the central PoST. The medium dashed line is the high-res fraction for the combined light gray PoSTs, and the long-dashed line is the high-res fraction for the combined dark gray PoSTs.

of the photons, and the dark gray PoSTs receive 4%. Assuming a 1000 μs time constant, we calculate the high resolution rate as a function of count rate for each PoST. The results are shown in Figure 8. Again we show the total high-res fraction in the solid black line, with the central, light gray, and dark gray PoSTs shown in short, medium, and long dashed lines, respectively. The high-res fraction drops to 50% around 120 counts per second, or at about 6 mCrab for a point source.

To calculate the 50% condition for extended sources, we consider flat field illumination. From Equation (1), for $R_{hr}/R_p = 0.5$, $f_{hr} = 20$, and $\tau = 1000$ μs, we obtain $R_p = 34.6$ counts/sec. If we assume 10-pixel long PoSTs, each PoST would cover 250 arcsec^2 (we assume each pixel on the PoST is a 5 arcsec square). The surface brightness of the object would have to be < 0.138 counts/arcsec^2/sec, or < 7 μCrab/arcsec^2/sec. The Perseus Cluster is 10 times dimmer than this limit, and would have a high-res fraction of 98%.

3.3. Energy Resolution

So far we have discussed the count rate performance of our proposed hybrid array. The downside to using these higher-multiplexing rows of SQUIDs and Position-sensitive devices is that both degrade the obtainable resolution. However, the degradation is not expected to be large, and we estimate that a resolution of 4–8 eV FWHM for the highly multiplexed PoSTs is achievable, at the same time as the central single-pixel array achieves resolutions of 2–4 eV. In fact, PoSTs have recently demonstrated energy resolutions of 8 eV FWHM at 6 keV.[7]

4. CONCLUSIONS

We have shown that a very conservative redesign of the current Constellation-X reference, with a 20×20 single-pixel TES core surrounded by a PoST array can increase the field of view of the Con-X microcalorimeter to at least 10 arcmin. The pileup in PoSTs for extended sources is shown to be negligible even for "bright" extended sources like the Perseus Cluster. Our approach is very conservative and does not significantly increase the cost or requirements of the Con-X microcalorimeter array, while maintaining the high throughput capability and increasing the FOV.

REFERENCES

1. N. E. White, H. D. Tananbaum, A. E. Hornschemeier, M. R. Garcia, R. Petre, and J. A. Bookbinder, "Constellation-x mission implementation approach and status," *SPIE Astronomical Telescopes and Instrumentation* **6266**(these proceedings), 2006.
2. M. R. Garcia, N. E. White, H. D. Tananbaum, R. Petre, A. E. Hornschemeier, and J. A. Bookbinder, "Science drivers for nasa's constellation x-ray mission," *SPIE Astronomical Telescopes and Instrumentation* **6266**(these proceedings), 2006.
3. P. Rosati, P. Tozzi, R. Giacconi, R. Gilli, G. Hasinger, L. Kewley, V. Mainieri, M. Nonino, C. Norman, G. Szokoly, J. X. Wang, A. Zirm, J. Bergeron, S. Borgani, R. Gilmozzi, N. Grogin, A. Koekemoer, E. Schreier, and W. Zheng, "The Chandra Deep Field-South: The 1 Million Second Exposure," *ApJ* **566**, pp. 667–674, Feb. 2002.
4. C. A. Kilbourne, S. R. Bandler, A. Brown, J. A. Chervenak, E. Figueroa-Feliciano, F. M. Finkbeiner, N. Iyomoto, R. L. Kelley, F. S. Porter, T. Saab, J. E. Sadleir, and J. White, "High-density arrays of x-ray microcalorimeters for constellation-x,," *SPIE Astronomical Telescopes and Instrumentation* **6266**(these proceedings), 2006.
5. W. B. Doriese, J. A. Beall, W. D. Duncan, L. Ferreira, G. C. Hilton, K. D. Irwin, C. D. Reintsema, J. N. Ullom, L. R. Vale, and Y. Xu, "Progress toward kilopixel arrays: 3.8 eV microcalorimeter resolution in 8-channel SQUID multiplexer," *Nuclear Instruments and Methods in Physics Research A* **559**, pp. 808–810, Apr. 2006.
6. N. Iyomoto, S. R. Bandler, R. P. Brekosky, J. A. Chervenak, E. Figueroa-Feliciano, F. M. Finkbeiner, R. L. Kelley, C. A. Kilbourne, M. A. Lindeman, K. Murphy, F. S. Porter, T. Saab, J. E. Sadleir, and D. J. Talley, "Position-sensitive transition-edge sensors," *Nuclear Instruments and Methods in Physics Research A* **559**, pp. 491–493, Apr. 2006.
7. E. Figueroa-Feliciano et al. *in preparation* .